

# Robust Sensor Fault Diagnosis by Multiple Model Approach

Sadegh Akbarpour, Mohammad Javad Khosrowjerdi \*

Faculty of Electrical Engineering, Sahand University of Technology, Tabriz, Iran.

E-mail: [khosrowjerdi@sut.ac.ir](mailto:khosrowjerdi@sut.ac.ir);

\*Corresponding author

Received: 22/04/2024, Revised:20/08/2024, Accepted: 28/09/2024.

## Abstract

This paper concerns the sensor faults diagnosis in the presence of unknown input, disturbances, actuator, and component faults using multiple linear model approaches in a group of complicated nonlinear systems. First, the sensor fault by adding a group of dynamic filters in the model output (hereinafter referred to as transfer filters) is arranged in additive form. Consequently, using a group of special linear Kalman filters a group of decoupled residuals are produced that only are dependent on sensor faults and noises. In continuing to distinguish the current operating point, by generating robust weighing coefficients an adaptive model and a stable adaptive filter are made that estimates the sensor fault in all operating areas. Finally, in a simulation environment, the competency of the proposed approach is evaluated.

**Keywords:** Fault diagnosis, Multiple models, Adaptive filters, and Gas turbine modeling.

## 1. Introduction

A fault is an unexpected deviation in the process variables from normal conditions that could lead to consequences resulting in loss of profit or design-based specifications. The fault based on the location can be classified as an actuator, component/process, and sensor/measure fault. In addition, based on behaviour as abrupt, incipient, and intermittent faults [1].

The results of a diagnostic system depend on achieving accurate operation information through sensors. Thus, it is necessary to determine whether the sensor faults and then reconstruct the failed sensor to reduce the impact on the performance of the diagnostic system. Conversely, the occurrence of component fault affects the sensor results. Therefore, the early identification of sensor faults is critical for making corrective actions to mitigate the impact [2, 3, 4, and 5].

Accurate modelling of a real system is difficult and the effect of unknown inputs, disturbances, and uncertainties could affect the system outputs. To eliminate the modelling errors and unknown disturbances affecting, unknown input observers (UIO) proposed that included disturbance decoupling conditions [6].

A reliable Fault Detection and Isolation (FDI) system requires an explicit consideration of the nonlinearities present in a system. There has been work on extending linear system approaches to non-linear systems about fault estimation for actuator/process faults in non-linear systems based on an adaptive estimator [7, 8].

However, for sensor fault estimation comparatively fewer results are available [9].

Also, there have been considered disturbances and uncertainties in the system to estimate the sensor fault [10, 11]. A systematic method to estimate the sensor fault that uses multiple observers was developed by linear UIO in nonlinear systems [12, 13] that, the actuator and sensor FDI problems have studied for a class of switched nonlinear systems with external disturbances. In summary, there is a lack of results on sensor fault estimation that apply to a general class of nonlinear systems without pre-assumption on the shape of the faults [14].

This paper proposes a method that sensor fault diagnosis is not sensitive to actuator and component faults and its main contribution is that, continuously and simultaneously estimates the vector of faults that is comprised of parameters whose indicate amount of deviation in a number of functional quantities in the system. We have not come across such an idea so far, so this could be a novelty. While, other methods detect the working mode of the system. They use the strategy of comparing and matching the status of system with the some parallel-simulated reference models. The models are derived for certain vectors of predefined deviations in several performance parameters in the system working conditions. Therefore if a model matches with the system status it is assumed related faults have been occurred [15].

This paper is organized as follows: In Section 2, the problem formulation and preliminaries have been defined

and formulated. Section 3 explains sensor fault diagnosis by multiple model approach. In Section 4, a case study on a twin-shaft gas turbine fault diagnosis by its thermodynamic modelling in the presence of faults, disturbances, unknown inputs, and noises is done. Following the conclusion is expressed in Section 5.

#### NOMENCLATURE

$cc, ct, pt$	combustion chamber, compressor turbine, power turbine
$K_{CC}, \Delta b$	Combustion chamber coefficients, pressure drop
$T, P, N, H$	Temperature (k), pressure (n/cm <sup>2</sup> ), rotational speed (rpm), health parameter
$\  \cdot \ _2, \cdot$	H <sup>2</sup> norm, First derivative
$LHV, J$	fuel low calorific (KJ/kg), inertia of shaft (kg.m <sup>2</sup> )
$\mathcal{N}$	Normal distribution
$F, f, g$	Nonlinear and polynomial functions
$R_g, \Gamma$	Universal gas constant, Constant
$\Sigma, \Pi$	Overall, Multiply
$\dot{m}, \dot{m}_a, \dot{m}_c$	mass flow, Air mass flow (kg/s), Compressor mass flow (kg/s)
$\eta$	isentropic efficiency
$\eta_{M_c}$	Compressor efficiency %
$w_f, UW$	Fuel kg/s, output work (Mj)
$V$	volume (m <sup>3</sup> )
$\alpha_{igv}, \alpha_{ngv}$	Opening angle of igv & ngv (%)
$c_p, c_v, c_{pg}$	specific constant-pressure and volume thermal capacity of air and gas (KJ/kg)
$T_s, k$	Sample time (second), iterative number
$i, j$	model and filter number indices

## 2. Problem formulation and preliminaries

For some dynamical systems, the nonlinear model, by considering the actuator, component, and sensor faults in the presence of unknown inputs and disturbances in a discrete-time base, may be defined as

$$\begin{aligned} \mathbf{x}_{k+1} &= \mathbf{F}(\mathbf{x}_k, \bar{\mathbf{u}}_k, \mathbf{H}_k, \mathbf{d}_k) + \boldsymbol{\theta}_k \\ \mathbf{y}_k &= \mathbf{G}(\mathbf{x}_k, \mathbf{z}_k) \end{aligned} \quad (1)$$

Where,  $\mathbf{x}_k \in \mathbb{R}^n$ ,  $\mathbf{y}_k \in \mathbb{R}^p$ ,  $\bar{\mathbf{u}}_k = [\mathbf{u}_k \ \mathbf{u}_k^f]^T \in \mathbb{R}^{m_1+m_2}$ ,  $\mathbf{H}_k \in \mathbb{R}^{q_1}$ ,  $\mathbf{d}_k \in \mathbb{R}^{q_3}$ ,  $\boldsymbol{\theta}_k \in \mathbb{R}^n$  and  $\mathbf{z}_k \in \mathbb{R}^{q_2}$  are vectors of states, outputs, augmented inputs, component faults, unknown inputs, disturbances and sensor faults. The augmented inputs  $\bar{\mathbf{u}}_k$  is comprised of the control inputs  $\mathbf{u}_k \in \mathbb{R}^{m_1}$  and the actuator faults  $\mathbf{u}_k^f \in \mathbb{R}^{m_2}$ . The functions  $\mathbf{F}$  and  $\mathbf{G}$  are assumed to be continuously differentiable. The linear state-space representation of (1) around the  $i^{th}$  operating point  $(\mathbf{x}_e^i, \bar{\mathbf{u}}_e^i, \mathbf{H}_e^i, \mathbf{z}_e^i)$ ,  $\forall i \in \{1, \dots, M\}$ , under stochastic assumptions, could be described by

$$\begin{aligned} \mathbf{x}_{k+1}^i &= \mathbf{A}_i \mathbf{x}_k^i + \mathbf{B}_i \bar{\mathbf{u}}_k + \mathbf{F}_i \mathbf{d}_k + \mathbf{E}_i \mathbf{H}_k + \boldsymbol{\Delta}_{X_i} + \boldsymbol{\omega}_k^i + \boldsymbol{\theta}_k \\ \mathbf{y}_k^i &= \mathbf{C}_i \mathbf{x}_k^i + \boldsymbol{\Delta}_{Y_i} + \mathbf{v}_k^i + \mathbf{S}_i \mathbf{z}_k \end{aligned} \quad (2)$$

where  $(\mathbf{A}_i, \mathbf{B}_i, \mathbf{C}_i)$  are state matrices,  $\mathbf{F}_i$ ,  $\mathbf{E}_i$  and  $\mathbf{S}_i$  are unknown input, component fault and sensor fault

contribution matrices with the appropriate dimensions.  $\boldsymbol{\Delta}_{X_i} = \mathbf{x}_e^i - \mathbf{A}_i \mathbf{x}_e^i - \mathbf{B}_i \mathbf{u}_e^i$ ,  $\boldsymbol{\Delta}_{Y_i} = \mathbf{y}_e^i - \mathbf{C}_i \mathbf{x}_e^i$  are modelling errors.  $\boldsymbol{\omega}_k^i$  with  $\mathbf{v}_k^i$  are the independent zero mean white noises by variance-covariance matrices,  $\mathbf{Q}_i$  and  $\mathbf{R}_i$ . The  $\mathbf{z}_i$  parameters serve as a signal that is added to or multiplied with the measurement variables, it may take on a constant or continuous form. The  $\mathbf{S}_i$  matrix reflects how the  $\mathbf{z}_i$  signals contribute to each output variable, based on the placement of the configured sensors in the system or the chosen output/measure quantities. Now by adding the following dynamic filters for each model in (2) the sensor fault from the system output is transferred to an augmented models' input (hereinafter refer as transfer filters).

$$\begin{aligned} \mathbf{x}_{k+1}^f &= \mathbf{A}_i^f \mathbf{x}_k^f + \mathbf{B}_i^f \mathbf{y}_k^i \\ \mathbf{y}_k^f &= \mathbf{C}_i^f \mathbf{x}_k^f \end{aligned} \quad (3)$$

which,  $(\mathbf{A}_i^f, \mathbf{B}_i^f, \mathbf{C}_i^f)$  are  $i^{th}$  transfer filters' state matrices with the appropriate dimension and  $\mathbf{x}_k^f \in \mathbb{R}^l$ ,  $\mathbf{y}_k^f \in \mathbb{R}^h$  are its state and outputs. Then the modified state space equations for  $i^{th}$  augmented model using the augmented state, faults, input, and outputs vectors as  $\tilde{\mathbf{x}}_k^i = [\mathbf{x}_k^i \ \mathbf{x}_k^f]^T$ ,  $\mathbf{H}_k^i = [\mathbf{d}_k \ \mathbf{H}_k \ \mathbf{z}_k \ \mathbf{u}_k^f]^T$ ,  $\tilde{\mathbf{y}}_k^i = \mathbf{y}_k^f$ ,  $\boldsymbol{\Delta}^i = [\boldsymbol{\Delta}_{X_i} \ \boldsymbol{\Delta}_{Y_i}]^T$  and  $\boldsymbol{\mu}_k^i = [\boldsymbol{\omega}_k^i \ \mathbf{v}_k^i]^T$  will be as:

$$\begin{aligned} \tilde{\mathbf{x}}_{k+1}^i &= \mathbf{A}_i' \tilde{\mathbf{x}}_k^i + \mathbf{B}_i' \mathbf{u}_k + \mathbf{E}_i' \mathbf{H}_k^i + \mathbf{W}_i' \boldsymbol{\Delta}^i + \mathbf{W}_i' \boldsymbol{\mu}_k^i + \mathbf{I}' \boldsymbol{\theta}_k \\ \tilde{\mathbf{y}}_k^i &= \mathbf{C}_i' \tilde{\mathbf{x}}_k^i \end{aligned} \quad (4)$$

that  $\mathbf{A}_i' \in \mathbb{R}^{(n+l) \times (n+l)}$ ,  $\mathbf{B}_i' \in \mathbb{R}^{(n+l) \times p}$ ,  $\mathbf{C}_i' \in \mathbb{R}^{h \times (n+l)}$ ,  $\mathbf{E}_i' \in \mathbb{R}^{(n+l) \times (m_1+q_1+q_2+q_3)}$ ,  $\mathbf{W}_i' \in \mathbb{R}^{(n+l) \times (n+p)}$ , and  $\mathbf{I}' \in \mathbb{R}^{(n+l) \times n}$  are the new state space, faults, noise and disturbance distribution matrices as the following forms

$$\begin{aligned} \mathbf{A}_i' &= \begin{pmatrix} \mathbf{A}_i & \mathbf{0} \\ \mathbf{B}_i^f \mathbf{C}_i & \mathbf{A}_i^f \end{pmatrix} & \mathbf{B}_i' &= \begin{pmatrix} \mathbf{B}_i \\ \mathbf{0} \end{pmatrix} & \mathbf{C}_i' &= \begin{pmatrix} \mathbf{0} & \mathbf{C}_i^f \end{pmatrix} \\ \mathbf{E}_i' &= \begin{pmatrix} \mathbf{F}_i & \mathbf{E}_i & \mathbf{0} & \mathbf{B}_i \\ \mathbf{0} & \mathbf{0} & \mathbf{B}_i^f \mathbf{S}_i & \mathbf{0} \end{pmatrix} & \mathbf{I}' &= \begin{pmatrix} \mathbf{I}_n & \mathbf{0} \\ \mathbf{0} & \mathbf{0} \end{pmatrix} & \mathbf{W}_i' &= \begin{pmatrix} \mathbf{I} & \mathbf{0} \\ \mathbf{0} & \mathbf{B}_i^f \end{pmatrix} \end{aligned} \quad (5)$$

here, the transfer filters shall be selected so that  $\mathbf{A}_i'$  becomes a Hurwitz matrix and all  $(\mathbf{A}_i', \mathbf{B}_i')$  with  $(\mathbf{A}_i', \mathbf{C}_i')$  become controllable and detectable.

## 3. Sensor Fault Diagnosis by Multiple Model approach

To establish a fault detector for the  $j^{th}$  augmented model in (4) a classical Kalman filter  $K_j^j$  is selected as the below

$$\begin{aligned} \hat{\mathbf{x}}_{k+1}^j &= \mathbf{A}_j' \hat{\mathbf{x}}_k^j + \mathbf{B}_j' \mathbf{u}_k + \mathbf{K}_j^j (\tilde{\mathbf{y}}_k^j - \hat{\mathbf{y}}_k^j) + \mathbf{W}_j' \boldsymbol{\Delta}^j \\ \hat{\mathbf{y}}_k^j &= \mathbf{C}_j' \hat{\mathbf{x}}_k^j \end{aligned} \quad (6)$$

that the state and output errors residuals  $\mathbf{e}^{i,j} = \tilde{\mathbf{x}}_k^i - \hat{\mathbf{x}}_k^j$ ,  $\mathbf{r}^{i,j} = \tilde{\mathbf{y}}_k^i - \hat{\mathbf{y}}_k^j$  between the  $j^{th}$  filter and augmented system in  $i^{th}$  operating point  $\forall i, j \in \{1 \dots M\}$ , are determined as

$$\begin{aligned} \mathbf{e}_{k+1}^{i,j} &= (\mathbf{A}_i' - \mathbf{K}_j^j \mathbf{C}_i') \tilde{\mathbf{x}}_k^i - (\mathbf{A}_j' - \mathbf{K}_j^j \mathbf{C}_j') \tilde{\mathbf{x}}_k^j + (\mathbf{B}_i' - \mathbf{B}_j') \mathbf{u}_k + \mathbf{E}_i' \mathbf{H}_k^i + \mathbf{W}_i' \boldsymbol{\mu}_k^i - \mathbf{W}_j' \boldsymbol{\Delta}^j + \mathbf{I}' \boldsymbol{\theta}_k \\ \mathbf{r}_{k+1}^{i,j} &= \mathbf{C}_i' \tilde{\mathbf{x}}_k^i - \mathbf{C}_j' \tilde{\mathbf{x}}_k^j \end{aligned} \quad (7)$$

$$\mathbf{r}_{k+1}^{i,j} = \mathbf{C}_i' \tilde{\mathbf{x}}_k^i - \mathbf{C}_j' \tilde{\mathbf{x}}_k^j \quad (8)$$

Now It is possible by defining  $\Delta \mathbf{A}'_{i,j} = \mathbf{A}'_i - \mathbf{A}'_j$ ,  $\Delta \mathbf{B}'_{i,j} = \mathbf{B}'_i - \mathbf{B}'_j$ ,  $\Delta \mathbf{C}'_{i,j} = \mathbf{C}'_i - \mathbf{C}'_j$ ,  $\Delta \mathbf{A}_{i,j} = \mathbf{W}'_i \Delta^i - \mathbf{W}'_j \Delta^j$  as the difference parameters between the augmented models and Kalman filters, rewrite (7) as the below

$$\mathbf{e}'_{k+1} = (\mathbf{A}'_i - \mathbf{K}'^j_k \mathbf{C}'_i) \mathbf{e}'_k + (\Delta \mathbf{A}_{i,j} - \mathbf{K}'^j_k \Delta \mathbf{C}_{i,j}) \hat{\mathbf{x}}^j_k + \Delta \mathbf{B}_{i,j} \mathbf{u}_k + \mathbf{E}'_i \mathbf{H}'_k + \Delta \mathbf{A}_{i,j} + \mathbf{W}'_i \mu_k + \mathbf{I}' \boldsymbol{\theta}_k \quad (9)$$

whereby taking into account the recursive form of (9) and assuming that the fault occurred at  $k_h$  and the system model (operating point) changes at  $k_m$ , ( $k_h, k_m < k$ ), by defining  $\Delta \mathbf{M}_k^{i,j} = (\Delta \mathbf{A}_{i,j} - \mathbf{K}'^j_k \Delta \mathbf{C}_{i,j}) \hat{\mathbf{x}}^j_k + \Delta \mathbf{B}_{i,j} \mathbf{u}_k + \mathbf{E}'_i \mathbf{H}'_k + \Delta \mathbf{A}_{i,j} + \mathbf{W}'_i \mu_k + \mathbf{I}' \boldsymbol{\theta}_k$ , (9) is rewritable in the form of

$$\mathbf{e}'_{k+1} = \sum_{v=k_h}^{k-1} (\Pi_{\Gamma=v}^k (\mathbf{A}'_i - \mathbf{K}'^j_{\Gamma} \mathbf{C}'_i) \mathbf{E}'_i \mathbf{H}'_v) + \mathbf{E}'_i \mathbf{H}'_k + \sum_{v=k_m}^{k-1} (\Pi_{\Gamma=v}^k (\mathbf{A}'_i - \mathbf{K}'^j_{\Gamma} \mathbf{C}'_i) \Delta \mathbf{M}_v^{i,j}) + \Delta \mathbf{M}_k^{i,j} + \sum_{v=k_h}^{k-1} (\Pi_{\Gamma=v}^k (\mathbf{A}'_i - \mathbf{K}'^j_{\Gamma} \mathbf{C}'_i) \mathbf{I}' \boldsymbol{\theta}_v + \mathbf{I}' \boldsymbol{\theta}_k + \mathbf{W}'_i \mu_k) \quad (10)$$

If in (10) the gain of the filters  $\mathbf{K}'^j_k$  in each iteration is selected so that simultaneously

$$(\mathbf{A}'_i - \mathbf{K}'^j_k \mathbf{C}'_i) \mathbf{E}'_i = 0, \forall i, j \in \{1, 2, \dots, M\} \quad (11)$$

and

$$(\mathbf{A}'_i - \mathbf{K}'^j_k \mathbf{C}'_i) \mathbf{I}' = 0, \forall i, j \in \{1, 2, \dots, M\} \quad (12)$$

then,  $\mathbf{e}'_{k+1}$  in (10) only will depend on  $\mathbf{E}'_i \mathbf{H}'_k$ ,  $+\mathbf{W}'_i \mu_k$  and  $\mathbf{I}' \boldsymbol{\theta}_k$  that will be isolated from the previous iteration and the fault effects. Therefore (7) and (8) in case of ( $i=j$ ) are changed to

$$\mathbf{e}'_{k+1} = \mathbf{E}'_i \mathbf{H}'_k + \mathbf{W}'_i \mu_k + \mathbf{I}' \boldsymbol{\theta}_k \quad (13)$$

Considering the dimension and format of  $\mathbf{C}'_i$ ,  $\mathbf{I}'$  and  $\mathbf{E}'_i$  from (5), then (13) is equal to

$$\mathbf{r}'_{k+1} = \begin{pmatrix} 0 & 0 & \mathbf{C}_i^f \mathbf{B}_i^f \mathbf{S}_i & 0 \end{pmatrix} \begin{pmatrix} \mathbf{d}_{k-1}^T \\ \mathbf{H}_{k-1}^T \\ \mathbf{z}_{k-1}^T \\ \mathbf{u}_{f_{k-1}}^T \end{pmatrix} + \begin{pmatrix} 0 & \mathbf{C}_i^f \mathbf{B}_i^f \end{pmatrix} \begin{pmatrix} \omega_k^T \\ \mathbf{v}_k^T \end{pmatrix} \quad (14)$$

Equation (14) proves that regarding the existence of unknown input, disturbance, component, and actuator faults only, the sensor fault consequences appear in the residuals  $\mathbf{r}'_{k+1}$  so, from (13) and (14) it is possible to estimate  $\mathbf{z}_k$  as the sensor fault by one step time delay in stochastic mode as the below

$$\hat{\mathbf{z}}_{k-1}^i = (\mathbf{C}_i^f \mathbf{B}_i^f \mathbf{S}_i)^{\dagger} (\mathbf{r}'_{k+1}^i - \mathbf{C}_i^f \mathbf{B}_i^f \mathbf{v}_k^i) \quad (15)$$

here  $(.)^{\dagger}$  denotes to the pseudo-inverse matrix and  $\hat{\mathbf{z}}_k^i$  is an estimation of  $\mathbf{z}_k$  by the  $i^{th}$  filter in its region. It is clear in the period that the plant takes on the  $i^{th}$  filters' model  $\hat{\mathbf{z}}_k^i$  adapts with  $\mathbf{z}_k$ , and then the fault will be made by consolidating  $M$  filter outputs.

### 3.1. Fault and Disturbance Mapping

To simultaneous satisfying the conditions in clauses (11) and (12) it is necessary the vector space of distribution matrices  $\mathbf{E}'_i$  and  $\mathbf{I}'$  are orthogonal complement of

$(\mathbf{A}'_i - \mathbf{K}'^i_k \mathbf{C}'_i) \forall i \in \{1, 2, \dots, M\}$ , though it is assumed for each augmented model two image mapping matrices  $\mathbf{O}_1^i$  and  $\mathbf{O}_2^i$  exist so that  $\mathbf{E}'_i \mathbf{O}_1^i = \mathbf{I}' \mathbf{O}_2^i = \mathbf{D}_i$  then (11) and (12) are rewritable as

$$(\mathbf{A}'_i - \mathbf{K}'^i_k \mathbf{C}'_i) \mathbf{E}'_i \mathbf{O}_1^i = 0, \forall i \in \{1, 2, \dots, M\} \quad (16)$$

and

$$(\mathbf{A}'_i - \mathbf{K}'^i_k \mathbf{C}'_i) \mathbf{I}' \mathbf{O}_2^i = 0, \forall i \in \{1, 2, \dots, M\} \quad (17)$$

Now it is possible by replacing  $\mathbf{E}'_i = \mathbf{D}_i \mathbf{O}_1^{i\dagger}$  and  $\mathbf{I}' = \mathbf{D}_i \mathbf{O}_2^{i\dagger}$  rewrite (4) as

$$\begin{aligned} \hat{\mathbf{x}}_{k+1}^i &= \mathbf{A}'_i \hat{\mathbf{x}}_k^i + \mathbf{B}'_i \mathbf{u}_k + \mathbf{D}_i \mathbf{O}_1^{i\dagger} \mathbf{H}'_k + \mathbf{W}'_i \Delta^i + \mathbf{W}'_i \mu_k + \mathbf{D}_i \mathbf{O}_2^{i\dagger} \boldsymbol{\theta}_k \\ \hat{\mathbf{y}}_k^i &= \mathbf{C}'_i \hat{\mathbf{x}}_k^i \end{aligned} \quad (18)$$

then by indicating  $\bar{\mathbf{H}}_k^i = \mathbf{O}_1^{i\dagger} \mathbf{H}'_k$  and  $\bar{\boldsymbol{\theta}}_k^i = \mathbf{O}_2^{i\dagger} \boldsymbol{\theta}_k$  (18) is modified as

$$\begin{aligned} \hat{\mathbf{x}}_{k+1}^i &= \mathbf{A}'_i \hat{\mathbf{x}}_k^i + \mathbf{B}'_i \mathbf{u}_k + \mathbf{D}_i \bar{\mathbf{H}}_k^i + \mathbf{W}'_i \Delta^i + \mathbf{W}'_i \mu_k + \mathbf{D}_i \bar{\boldsymbol{\theta}}_k^i \\ \hat{\mathbf{y}}_k^i &= \mathbf{C}'_i \hat{\mathbf{x}}_k^i \end{aligned} \quad (19)$$

$\bar{\mathbf{H}}_k^i$  and  $\bar{\boldsymbol{\theta}}_k^i$  are images of augmented faults vector  $\mathbf{H}'_k$  and disturbance vector  $\boldsymbol{\theta}_k$ . To avoid the removing of  $\mathbf{H}'_k$  or  $\boldsymbol{\theta}_k$  elements effecting at the augmented models, in selection of  $\mathbf{O}_1^i$  and  $\mathbf{O}_2^i$  shall be consider that  $\mathbf{D}_i$  is full rank and the rank of matrices  $\mathbf{D}_i \mathbf{O}_1^{i\dagger}$  and  $\mathbf{D}_i \mathbf{O}_2^{i\dagger}$  are same as the length of vectors  $\mathbf{H}'_k$  and  $\boldsymbol{\theta}_k$ . By this way if the filter  $\mathbf{K}'^i_k$  is designed so that, could provide the condition

$$(\mathbf{A}'_i - \mathbf{K}'^i_k \mathbf{C}'_i) \mathbf{D}_i = 0, \forall i \in \{1, 2, \dots, M\} \quad (20)$$

then both conditions in clauses (11) and (12) are satisfied.

### 3.2. Kalman Filter

A solution to algebraic constraints (20) for each filter was proposed in [16] with parameterization of the Kalman filters  $\mathbf{K}'^i_k$  as

$$\mathbf{K}'^i_k = \boldsymbol{\omega}'_i \boldsymbol{\Xi}'_i + \bar{\mathbf{K}}'^i_k \boldsymbol{\Xi}'_i \quad (21)$$

here in (25)  $\boldsymbol{\omega}'_i = \mathbf{A}'_i \mathbf{D}_i$ ,  $\boldsymbol{\Xi}'_i = (\mathbf{C}'_i \mathbf{D}_i)^{\dagger}$ ,  $\boldsymbol{\Xi}'_i = \boldsymbol{\alpha}'_i (\mathbf{I}_{(n+l)} - \mathbf{C}'_i \mathbf{D}_i \boldsymbol{\Xi}'_i)$  that,  $\boldsymbol{\alpha}'_i$  is an arbitrary matrix is determined so that the matrix  $\boldsymbol{\Xi}'_i$  to be full rows rank and,  $\bar{\mathbf{K}}'^i_k$  is a degree of freedom in filter design and is used to stabilizing the filter. According to [17] to guarantee the filter stability the gain of  $\bar{\mathbf{K}}'^i_k$  is determined as

$$\begin{aligned} \bar{\mathbf{K}}'^i_k &= \bar{\mathbf{A}}_i \bar{\mathbf{P}}_k^i \bar{\mathbf{C}}_i^T (\bar{\mathbf{A}}_i \bar{\mathbf{P}}_k^i \bar{\mathbf{C}}_i^T + \bar{\mathbf{V}}_i)^{-1} \\ \bar{\mathbf{P}}_{k+1}^i &= (\bar{\mathbf{A}}_i - \bar{\mathbf{K}}'^i_k \bar{\mathbf{C}}_i) \bar{\mathbf{P}}_k^i (\bar{\mathbf{A}}_i - \bar{\mathbf{K}}'^i_k \bar{\mathbf{C}}_i)^T + \bar{\mathbf{K}}'^i_k \bar{\mathbf{V}}_i (\bar{\mathbf{K}}'^i_k)^T + \bar{\mathbf{Q}}_i \end{aligned} \quad (22)$$

with  $\bar{\mathbf{A}}_i = (\mathbf{A}'_i - \boldsymbol{\omega}'_i \boldsymbol{\Xi}'_i \mathbf{C}'_i)$ ,  $\bar{\mathbf{C}}_i = \boldsymbol{\Xi}'_i \mathbf{C}'_i$ ,  $\bar{\mathbf{V}}_i = \boldsymbol{\Xi}'_i \mathbf{R}_i \boldsymbol{\Xi}'_i^T$  and  $\bar{\mathbf{Q}}_i = \mathbf{Q}_i + \boldsymbol{\omega}'_i \boldsymbol{\Xi}'_i \mathbf{R}_i \boldsymbol{\Xi}'_i^T$

### 3.3. Adaptive Model

At this stage, to find the compatible linear model to the plant at any time by multiplying  $\boldsymbol{\Xi}'_j$  on both sides of (13)

$\boldsymbol{\gamma}_{k+1}^{i,j}$  as decoupled residuals are generated by

$$\boldsymbol{\gamma}_{k+1}^{i,j} = \boldsymbol{\Xi}'_j \mathbf{r}'_{k+1}^i = \boldsymbol{\Xi}'_j \mathbf{C}'_i \mathbf{E}'_i \mathbf{H}'_{k-1} + \boldsymbol{\Xi}'_j \mathbf{C}'_i \mathbf{W}'_i \mu_k \quad (23)$$

Due to the matrix properties (if,  $i=j$ ) then  $(\boldsymbol{\Xi}'_j \mathbf{C}'_i \mathbf{E}'_i = 0)$

and  $(\Xi'_j \mathbf{C}'_i \mathbf{I}' = 0)$  then  $\mathbf{y}'^{i,i}_k = \Xi'_j \mathbf{C}'_i \mathbf{W}'_i \mu^i_k$  that is a Gaussian term [18]. It means that the Gaussian format of  $\mathbf{y}'^{i,i}_k$  at any time for any filter not only approves the conformity of its model with the operating point but also, this property only for one filter will be valid because all linear models are different from together. Now by using this specification a model identifier method in each iteration is configured by developing an adaptive model as the following form [18].

$$\begin{aligned} \mathbf{x}^*_{k+1} &= \mathbf{A}^*_k \mathbf{x}_k + \mathbf{B}^*_k \mathbf{u}_k + \mathbf{E}^*_k \mathbf{H}'_k + \mathbf{A}^*_k \mathbf{I}' \boldsymbol{\theta}_k \\ \mathbf{y}^*_k &= \mathbf{C}^*_k \mathbf{x}_k \end{aligned} \quad (24)$$

where  $\mathbf{x}^*_k$  and  $\mathbf{y}^*_k$  are the plant states and outputs, and the time variable state space matrices are,  $\mathbf{A}^*_k = \sum_{i=1}^M \lambda^i_k \mathbf{A}'_i$ ,  $\mathbf{B}^*_k = \sum_{i=1}^M \lambda^i_k \mathbf{B}'_i$ ,  $\mathbf{C}^*_k = \sum_{i=1}^M \lambda^i_k \mathbf{C}'_i$ ,  $\mathbf{E}^*_k = \sum_{i=1}^M \lambda^i_k \mathbf{E}'_i$ ,  $\mathbf{W}^*_k = \sum_{i=1}^M \lambda^i_k \mathbf{W}'_i \Delta^i$  and, the coefficients  $\lambda^i_k$  are called probability distribution functions [19], are as the below

$$\lambda^i_{k+1} = \frac{\lambda^i_k (l^i_k)^{-1}}{\sum_{h=1}^M \lambda^i_h (l^i_h)^{-1}} \quad (25)$$

where  $l^i_k$  is called the distance function between the plant and  $i^{th}$  linear augmented model in (4) and is described as the below

$$l^i_k = \sum_{n=k-t_0}^n \|\mathbf{y}'^{i,i}_n\|_2 \quad (26)$$

here  $k$  is the current iteration number and,  $t_0$  is the length of comparison period [26].

### 3.4. Adaptive Filters

For the fault estimation in a dynamic system as (24), an adaptive filter with gain  $\mathbf{K}_k$  can be configured as

$$\begin{aligned} \tilde{\mathbf{x}}_{k+1} &= \mathbf{A}^*_k \tilde{\mathbf{x}}_k + \mathbf{B}^*_k \mathbf{u}_k + \mathbf{K}_k (\mathbf{y}^*_k - \tilde{\mathbf{y}}_k) + \mathbf{A}^*_k \\ \tilde{\mathbf{y}}_k &= \mathbf{C}^*_k \tilde{\mathbf{x}}_k \end{aligned} \quad (27)$$

To provide the conditions of clause (20) in (24)  $\mathbf{D}^*_k$  is described as  $\mathbf{D}^*_k = \mathbf{E}^*_k \mathbf{O}^1_k = \mathbf{I}' \mathbf{O}^2_k$  then  $\bar{\mathbf{H}}_K = \mathbf{O}^1_k{}^\dagger \mathbf{H}'_k$  and  $\bar{\boldsymbol{\theta}}_K = \mathbf{O}^2_k{}^\dagger \boldsymbol{\theta}_k$  by defining  $\boldsymbol{\omega}_k = \mathbf{A}^*_k \mathbf{D}^*_k$ ,  $\Psi_k = (\mathbf{C}^*_k \mathbf{D}^*_k)^\dagger$ ,  $\Xi_k = \boldsymbol{\alpha} (\mathbf{I}_m - \mathbf{C}^*_k \mathbf{D}^*_k \Psi)$  that, absolut matrix  $\boldsymbol{\alpha}$  is defined so that  $\Xi_k$  to become full row rank. Then the filters  $\mathbf{K}_k$  is decomposed as the below

$$\mathbf{K}_k = \boldsymbol{\omega}_k \Psi_k + \bar{\mathbf{K}}_K \Xi_k \quad (28)$$

The estimation error and output residuals in (24) by including (28) is expressed as

$$\begin{aligned} \mathbf{e}_{k+1} &= (\mathbf{A}^*_k - \mathbf{K}_k \mathbf{C}^*_k) \mathbf{e}_k + \mathbf{D}^*_k \bar{\mathbf{H}}_K + \mathbf{D}^*_k \bar{\boldsymbol{\theta}}_K = (\mathbf{A}^*_k - (\boldsymbol{\omega}_k \Psi_k + \bar{\mathbf{K}}_K \Xi_k) \mathbf{C}^*_k) \mathbf{e}_k + \mathbf{D}^*_k \bar{\mathbf{H}}_K + \mathbf{D}^*_k \bar{\boldsymbol{\theta}}_K = (\mathbf{A}^*_k (\mathbf{I} - \mathbf{D}^*_k \Psi_k \mathbf{C}^*_k) - \bar{\mathbf{K}}_K \Xi_k \mathbf{C}^*_k) \mathbf{e}_k + \mathbf{D}^*_k \bar{\mathbf{H}}_K + \mathbf{D}^*_k \bar{\boldsymbol{\theta}}_K \end{aligned} \quad (29)$$

$$\mathbf{r}_k = \mathbf{C}^*_k \mathbf{e}_k \quad (30)$$

By defining  $\ddot{\mathbf{A}}^*_k = \mathbf{A}^*_k (\mathbf{I} - \mathbf{D}^*_k \Psi_k \mathbf{C}^*_k) = \sum_{i=1}^M \lambda^i_k \mathbf{A}'_i (\mathbf{I} - \mathbf{D}^*_k \Psi_k \mathbf{C}^*_k)$  and  $\ddot{\mathbf{C}}^*_k = \Xi_k \mathbf{C}^*_k$  then the relation (29) changes to:

$$\mathbf{e}_{k+1} = (\ddot{\mathbf{A}}^*_k - \bar{\mathbf{K}}_K \ddot{\mathbf{C}}^*_k) \mathbf{e}_k + \mathbf{D}^*_k \bar{\mathbf{H}}_K + \mathbf{D}^*_k \bar{\boldsymbol{\theta}}_K \quad (31)$$

If (31) or the adaptive filter is become stable then (30) changes to

$$\mathbf{r}_k = \mathbf{C}^*_k (\mathbf{D}^*_k \bar{\mathbf{H}}_K + \mathbf{D}^*_k \bar{\boldsymbol{\theta}}_K) \quad (32)$$

The ultimate estimation of sensor fault by considering that  $\mathbf{C}^*_k \mathbf{D}^*_k \bar{\boldsymbol{\theta}}_K = 0$  using the relations (23) and (32) in detection filters is summarized as

$$\tilde{\mathbf{z}}_{k-1} = (\mathbf{C}^*_k \mathbf{f}^* \mathbf{B}_k \mathbf{f}^* \mathbf{S}_k)^{\dagger} (\mathbf{r}_k) \quad (33)$$

here  $\mathbf{r}_k = \mathbf{y}^*_k - \tilde{\mathbf{y}}_k$  is adaptive filter residuals and  $(\cdot)_k^{\dagger} = \sum_{i=1}^M \lambda^i_k (\cdot)_i^{\dagger}$  with  $\mathbf{S}_k^* = \sum_{i=1}^M \lambda^i_k \mathbf{S}_i$  that  $\tilde{\mathbf{z}}_{k-1}$  is an estimation of sensor faults by one sample time delay.

### 3.5. Filters Stability

To guarantee the stability of the adaptive filters in (27) the gains  $\bar{\mathbf{K}}_K$  in (28) according to the Lyapunov theorem [20] shall be determined so that the following inequities to be valid.

$$(\ddot{\mathbf{A}}^*_k - \bar{\mathbf{K}}_K \ddot{\mathbf{C}}^*_k) \mathbf{P}'_k (\ddot{\mathbf{A}}^*_k - \bar{\mathbf{K}}_K \ddot{\mathbf{C}}^*_k)^T - \mathbf{P}'_k < 0, \mathbf{P}'_k > 0 \quad (34)$$

The inequalities (34) by using Schur complement and the variable changing as  $\bar{\mathbf{K}}_K = \mathbf{P}'^{-1}_k \mathbf{R}'^i_k$  are transformed to linear matrix inequality (LMI) in the form of

$$\begin{pmatrix} \mathbf{P}'_k & \ddot{\mathbf{A}}^{*T}_k \mathbf{P}'_k - \ddot{\mathbf{C}}^{*T}_k \mathbf{R}'^i_k{}^T \\ \mathbf{P}'_k \ddot{\mathbf{A}}^*_k - \mathbf{R}'^i_k \ddot{\mathbf{C}}^*_k & \mathbf{P}'_k \end{pmatrix} > 0 \quad (35)$$

By replacing  $\ddot{\mathbf{A}}^*_k$  with decryptions and decomposing  $\mathbf{R}'_k$  as  $\mathbf{R}'_k = \sum_{i=1}^M \lambda^i_k \mathbf{R}'^i_k$  then (35) are converted to “(see (36))” Due to the relations (35) and (36) and although considering that  $\sum_{i=1}^M \lambda^i_k = 1$  then LMI (36) is decomposed to “(see (37))” The LMI (37) will be true if each of its elements are Positive. Finally, by resolving the  $M$  number of LMIs  $\mathbf{R}'_i$  are produced. So by developing  $\mathbf{R}'_i$  the gain  $\bar{\mathbf{K}}_K$  is achieved.

$$\begin{pmatrix} \mathbf{P}'_k & \sum_{i=1}^M \lambda^i_k [(\mathbf{A}'_i (\mathbf{I} - \mathbf{D}^*_k \Psi_k \mathbf{C}^*_k))^T \mathbf{P}'_k - \ddot{\mathbf{C}}^{*T}_k \mathbf{R}'^i_k{}^T] \\ \sum_{i=1}^M \lambda^i_k [\mathbf{P}'_k \mathbf{A}'_i (\mathbf{I} - \mathbf{D}^*_k \Psi_k \mathbf{C}^*_k) - \mathbf{R}'^i_k \ddot{\mathbf{C}}^*_k] & \mathbf{P}'_k \end{pmatrix} > 0 \quad (36)$$

$$\sum_{i=1}^M \lambda^i_k \begin{pmatrix} \mathbf{P}'_k & (\mathbf{A}'_i (\mathbf{I} - \mathbf{D}^*_k \Psi_k \mathbf{C}^*_k))^T \mathbf{P}'_k - \ddot{\mathbf{C}}^{*T}_k \mathbf{R}'^i_k{}^T \\ \mathbf{P}'_k \mathbf{A}'_i (\mathbf{I} - \mathbf{D}^*_k \Psi_k \mathbf{C}^*_k) - \mathbf{R}'^i_k \ddot{\mathbf{C}}^*_k & \mathbf{P}'_k \end{pmatrix} > 0 \quad (37)$$

### 3.6. Algorithm

Finally, to design a diagnostic system according to the proposed approach, the following steps are performed:

1. The comprehensive nonlinear model of the system is developed.
2. The linearized models (2) in some operating points is developed. The operating points by equal intervals on the input range are selected.
3. The sensor fault transfer filters in (3) are selected, and related augmented models in (4) are established.
4. The matrices  $\mathbf{O}_1^i$  and  $\mathbf{O}_2^i$  with  $\mathbf{D}_i$  are calculated and the coefficients  $\bar{\mathbf{K}}_k^i$  as (21) are provided.
5. The sensor faults detection filters  $\mathbf{K}_k^i$  for each augmented model in (4) according to (6) are configured.
6. Residuals  $\mathbf{r}_k^{i,i}$  in (13) and decoupled residuals  $\mathbf{Y}_k^{i,j}$  as (23) are calculated.
7. Continuously a group of sensor faults vectors  $\tilde{\mathbf{z}}_{k-1}^i$  by each  $i^{th}$  detection filter as (15) are generated.
8. If at a moment, the  $j^{th}$  filter decoupled residuals vector  $\mathbf{Y}_k^{i,j}$  take in the Gaussian format then  $\tilde{\mathbf{z}}_{k-1}^i$  could be considered as the plant fault.
9. The coefficients  $\lambda_k^i$  as (25) using  $\mu_k^i$  in (26) are produced.
10. The adaptive model in (24) for the sensor fault estimator are shaped.
11.  $\mathbf{R}_k^i \forall i \in \{1, 2, \dots, M\}$  by resolving  $M$  number of LIMs in (37) are acquired then,  $\mathbf{R}'_k = \sum_{i=1}^M \lambda_k^i \mathbf{R}_k^i$  is obtained and, the gains  $\mathbf{K}'_k = \mathbf{P}'_k \mathbf{R}'_k$  are developed.
12. The adaptive sensor faults detection filter  $\mathbf{K}_k$  in (27) by using  $\mathbf{K}'_k$  in (28) are configured.

13. The adaptive residuals  $\mathbf{r}_k$  in (30) are generated and,  $\mathbf{z}_{k-1}$  as (33) are estimated.

### 4. A case study: Gas Turbine

The scheme of a stationary twin-shaft gas turbine engine as shown in Fig 1 consists of various components that are linked together. Gas turbine performance estimation depends on the detailed information of component maps that, in equations are presented by  $\dot{m}_c$ ,  $\eta_{M_c}$ ,  $\dot{m}_{ct}$ ,  $\eta_{c_t}$ ,  $\dot{m}_{pt}$  and  $\eta_{pt}$  which are nonlinear polynomial functions [21, 22, 23, and 24].

Usually the components' faults consequences are considered by defining health indicator variables [25, 26] then,

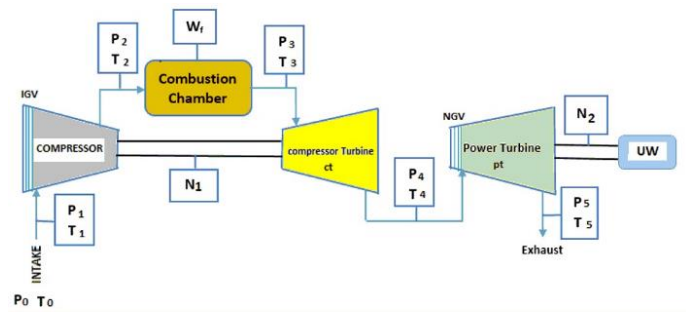


Fig 1. Main parts of a twin shaft industrial gas turbine

by defining  $\mathbf{H} = [H_{\dot{m}_c} H_{\eta_{M_c}} H_{\dot{m}_{ct}} H_{\eta_{c_t}} H_{\dot{m}_{pt}} H_{\eta_{pt}}]^T$  as health indicator vector and selecting the states and inputs  $\mathbf{x} = [N_1 N_2 T_3 P_4 P_5 P_6]^T$ ,  $\mathbf{u} = [w_f a_{igv} a_{ngv}]$  the comprehensive reconfigured partial differential equations in form  $\dot{\mathbf{X}} = \mathbf{F}(\mathbf{x}, \mathbf{u}, \mathbf{H})$  at the continuous time base is developed as the below “(see (38))” for the more detail about the dynamic modelling please refer to [8].

$$\begin{pmatrix} \dot{N}_1 \\ \dot{N}_2 \\ \dot{T}_3 \\ \dot{P}_3 \\ \dot{P}_4 \\ \dot{P}_5 \end{pmatrix} = \begin{pmatrix} \left[ \frac{30}{\pi} \right]^2 \frac{1}{J_1 N_1} \left[ H_{\dot{m}_{ct}} \dot{m}_{ct} H_{\eta_{c_t}} \eta_{c_t} c_{pg} (T_3 - T_4) - H_{\dot{m}_c} \dot{m}_c H_{\eta_{M_c}} \eta_{M_c} c_{pa} (T_2 - T_1) \right] \\ \left[ \frac{30}{\pi} \right]^2 \frac{1}{J_2 N_2} \left[ \dot{m}_{pt} H_{\dot{m}_{pt}} \eta_{pt} H_{\eta_{pt}} c_{pg} (T_4 - T_5) - UW \right] \\ \frac{R_g T_3}{P_3 V_1 c_{vg}} \left[ K \left( c_{pg} T_2 H_{\dot{m}_c} \dot{m}_c + LHV \eta_{cc} w_f - c_{pg} T_3 \dot{m}_{ct} H_{\dot{m}_{ct}} \right) - c_{pg} T_3 (H_{\dot{m}_c} \dot{m}_c + w_f - \dot{m}_{ct} H_{\dot{m}_{ct}}) \right] \\ \frac{P_3}{T_3} \dot{T}_3 + \frac{R_g T_3 (H_{\dot{m}_c} \dot{m}_c + w_f - H_{\dot{m}_{ct}} \dot{m}_{ct})}{V_1} \\ \frac{R_g T_4 (H_{\dot{m}_{ct}} \dot{m}_{ct} - \dot{m}_{pt} H_{\dot{m}_{pt}})}{V_2} \\ \frac{R_g T_5 (\dot{m}_{pt} H_{\dot{m}_{pt}} - \Gamma \sqrt{P_5})}{V_3} \end{pmatrix} \quad (38)$$

## 5. Simulation

The necessary data gathered from a prototype gas turbine (GE10.b). A log of measured outputs provided, and in some operating points, dynamic states and the other necessary parameters for developing the linear models calculated that are listed in Table 1. The simulated disturbances and used unknown input with the assumed component and actuator faults in Fig. 2 are shown.

The required coefficients, states, and fault contribution matrices in discrete time bases with the transfer filters are noted in the appendix.

For simplicity, the unknown input assumed the atmospheric pressure ( $P_1$ ). The component faults are assumed as deviations in the compressor air mass flow rate and compressor's turbine efficiency ( $H_{\dot{m}_c}$ ,  $H_{\eta_{ct}}$ ) and, in the actuators, the deviation in  $\alpha_{igv}$  position is considered and, in the sensor fault the deviation in the second shaft speed measuring and combustor temperature ( $z_{2k}$  and  $z_{3k}$ ) are investigated. Here, the nonlinear model as a plant is replaced by the piecewise linear model, though in each specified part of the operating region, the related linear model is used as the plant model; each region takes up to 300 sample times with  $T_s=0.1$  s (30 seconds). This study is conducted by MATLAB 2020b and, by using the first-order Euler method [27] the continuous nonlinear model discretised.

**Results:** In Fig 3, the generated and estimated sensor faults (a) via their root mean square errors (RMSE) (b) are illustrated. The fault in the second sensor ( $z_2$ ) is assumed to be a drift and about 4% of its full range, and in the third sensor ( $z_3$ ), assumed to be in the form of a three-step between  $\pm 4\%$  of its full range. As seen in (a) the estimation of each filter in duration that the system takes on that filter model converges to the faults, but in the other regions, the estimation error increases, and estimation may diverge.

However, the accuracy of the estimation will depend on the transfer filter selection. Although the shape of RMSE curves for all filters during their mode matching with the system are the same but its altitude are considerable.

**Comparison:** Compared to other fault estimation methods for gas turbines, the proposed approach in this article utilizes continuous matching between model bank models and the real system. This allows it to effectively encompass the performance of various fault diagnosis methods, such as those in [14]. When a model aligns with the system's state, the estimated fault signals for its filter will be Gaussian; otherwise, they will not. In contrast, other methods typically employ mode identification, requiring a model bank with different predefined faults. As the gas turbine transitions between healthy and faulty modes, this method can identify the appropriate model, enabling the determination of the system's health or the type of fault

based on the cause-and-effect table.

Table 1. GE- GT10/2 Gas turbine's initial data at the selected operating point

	Point 1	Point 1	Point 1	Point 1
UW%	50	55	54.7	71
$\alpha_{igv}\%$	62	84	95	94
$\alpha_{ngv}\%$	0.1	0.2	0	0.4
$N_2$ (rpm)	9938	10275	10462	11000
$N_1$ (rpm)	5525	6600	7500	7150
$C_p$	1.047	1.053	1.053	1.068
$C_{pa}$	1.047	10.53	1.058	1.068
$\eta_c\%$	87.4	79.3	88.6	88.5
$\eta_{ct}\%$	58	60	61	61
$\dot{m}_f$ (Kg/s)	0.29	0.39	0.45	0.49
$\dot{m}_c$ (Kg/s)	35	39.5	44	50
$T_1$ (c)	1	-1	3	29
$T_2$ (c)	301	338	360	420
$T_3$ (c)	653	762	808	835
$P_1$ (Bar)	0.83	0.83	0.83	0.83
$P_2$ (Bar)	8.7	9.2	12	11.7
$P_3$ (Bar)	8.3	8.7	11.4	11.1
$P_4$ (Bar)	5.75	6.12	7.98	7.78

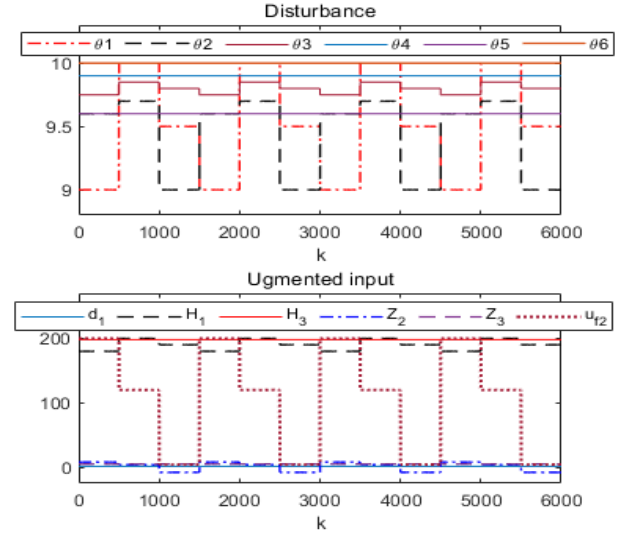


Fig 2. Disturbance, faults and unknown input

Compressor and turbine map slopes on operating points are as:

$$\begin{aligned} \frac{\partial \eta_{ct}}{\partial P_3} &= 0.2, \frac{\partial \eta_{ct}}{\partial N_1} = 0.2, \frac{\partial \dot{m}_{ct}}{\partial P_4} = 0.15, \frac{\partial \dot{m}_{ct}}{\partial P_3} = 0.25, \frac{\partial \dot{m}_{ct}}{\partial N_1} = 0.1, \frac{\partial \dot{P}_3}{\partial P_4} = 1, \frac{\partial \dot{P}_3}{\partial N_1} = \\ &0.1, \frac{\partial \dot{m}_{ct}}{\partial \alpha_{igv}} = 0.5, \frac{\partial \dot{m}_c}{\partial \alpha_{igv}} = 1, \frac{\partial \eta_{pt}}{\partial \alpha_{igv}} = 0.1, \frac{\partial \dot{m}_{pt}}{\partial \alpha_{igv}} = 0.8, \frac{\partial \dot{m}_{pt}}{\partial w_f} = 0.01, \frac{\partial \dot{m}_{ct}}{\partial w_f} = 0.01, \\ \frac{\partial UW}{\partial N_2} &= 3, \frac{\partial \eta_{pt}}{\partial N_2} = 0.1, \frac{\partial \eta_{pt}}{\partial P_5} = 0.5, \frac{\partial \dot{m}_{pt}}{\partial P_4} = 0.1, \frac{\partial \dot{m}_{ct}}{\partial w_f} = 0.01, \frac{\partial \eta_{pt}}{\partial \alpha_{igv}} = 0.1, \frac{\partial \dot{m}_c}{\partial N_1} = 1, \\ \frac{\partial \dot{m}_{ct}}{\partial N_1} &= -0.1, \frac{\partial \dot{m}_{pt}}{\partial N_2} = 0.1, \frac{\partial \dot{m}_{pt}}{\partial P_5} = -0.1 \end{aligned}$$

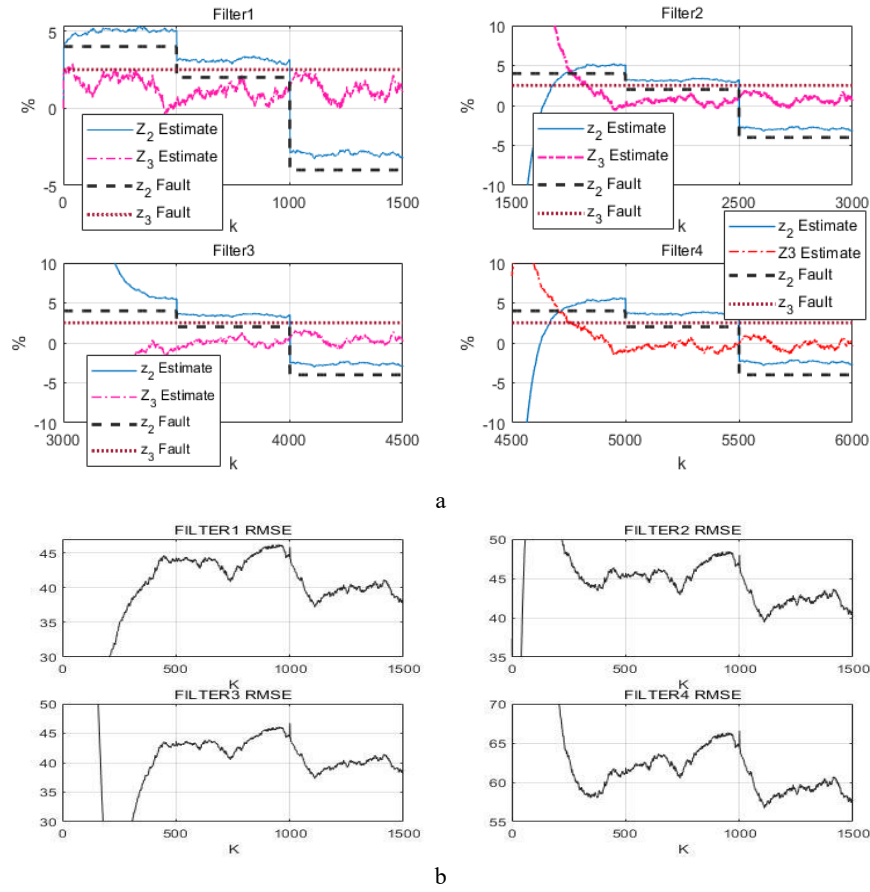


Fig 3. Sensor fault and its estimation via RMSE by each filter (a-Estimation, b-RMSE)

Decoupled residuals  $\gamma_k^{i,i}$  in Fig 4 is illustrated as it is seen each filter decoupled residuals when the system takes that filter model has Gaussian format and in the other region it

is not. By using this specification and generating two robust coefficients as distance and probability distribution functions, the adaptive model is configured.

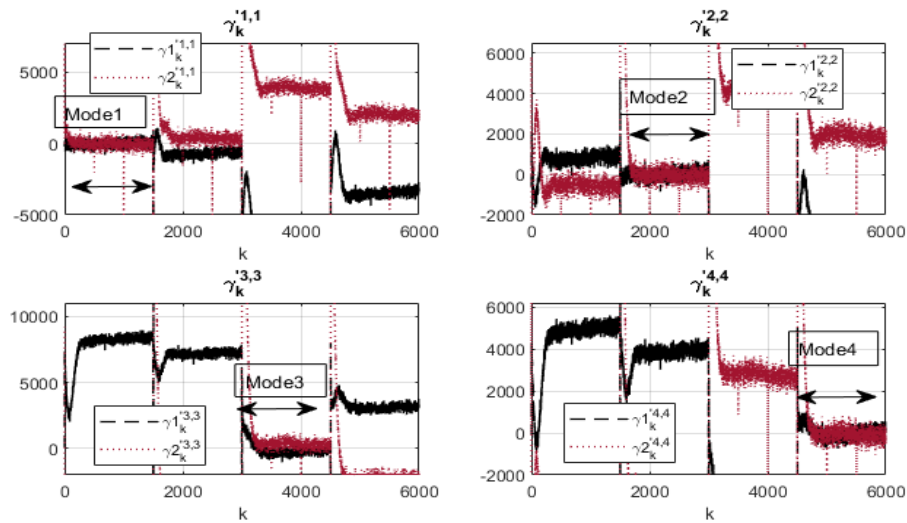


Fig 4. Decoupled residuals  $\gamma_k^{i,i}$  during the simulation time



The inverse of distance functions and probability distribution functions of models in Fig 5 against the system during all operating areas is shown. As it is obvious when

system modes switch from a mode to the next state these parameters are able to measure and show the current operating point and consequently the model of the system.

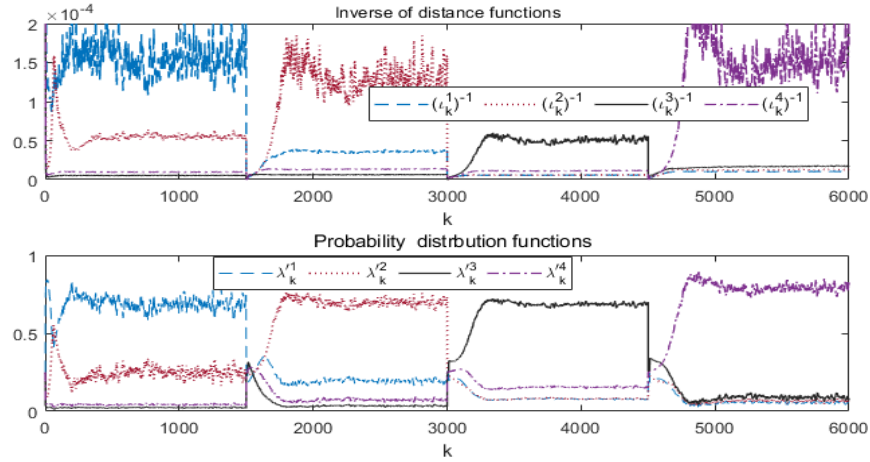


Fig 5. Distance functions and probability distribution of models

In Fig 6 the adaptive estimator, performance (a) via the estimates RMSE (b) is shown. The method's efficiency is

acceptable whether the behaviour of the faults and selecting the matrices  $O_1^i$  and  $O_2^i$  or  $O_k^1$  and  $O_k^2$  affect the results.

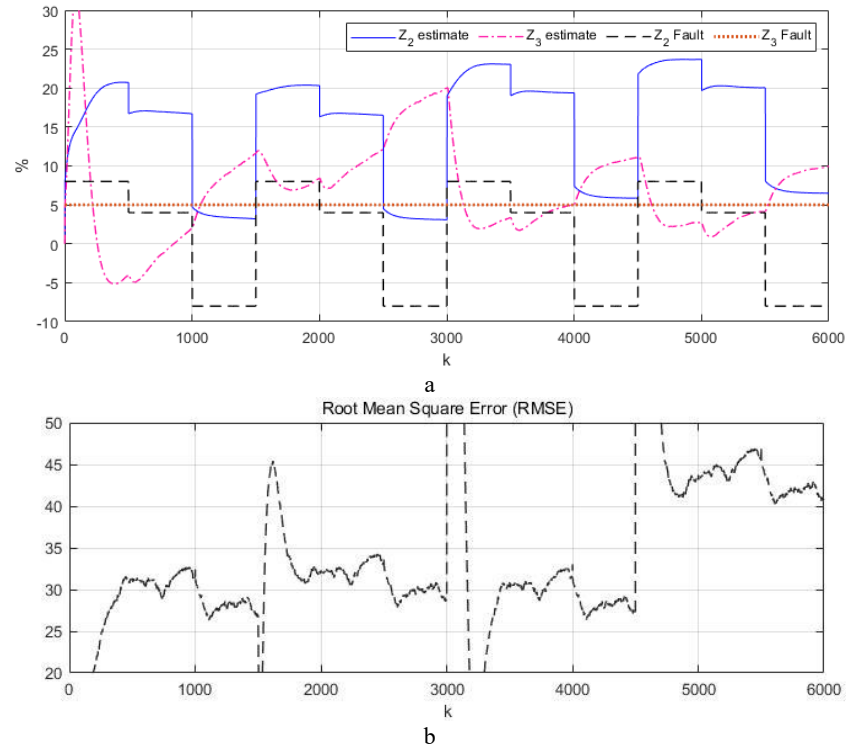


Fig 6. Adaptive estimator performance via its RMSE (a-Estimation, b-RMSE)

## 6. Conclusion

The proposed multiple model-based method in this paper could detect and diagnose the sensor faults at the nonlinear

systems in the presence of disturbances, unknown inputs, and other faults. In this method, the annoying inputs and faults are organized and integrated into an augmented



vector. By linear mapping of this vector together with the disturbance vector on a new mapping plane, the sensor faults are decoupled from them. Then by the filter decomposition strategy, some robust weighing coefficients are generated to construct the adaptive redundant model, and, by developing a related adaptive filter as an estimator, the sensor faults are estimated. The accuracy of the method depends on selecting the transferring filters and the image mapping matrices of disturbance and augmented vector that, estimation RMSE both for classic and adaptive filters approves this clause. As the results of the simulation in the figures, the estimation of dynamic fault traceability is better than the freeze or fixed faults. If the rank of the mapping matrices becomes less than the number of integrated vector lengths or the number of disturbance elements then the decoupling of some arrays from the annoying inputs or disturbance vectors from the sensor faults may be lost and, the results will be chaotic. In addition, The complexity and large number of mathematical relationships and the real-time condition of LMI to ensure stability cause a high volume of calculations, which requires fast and up-to-date controllers. The case study results proved that this approach could be used in this kind of nonlinear system.

## References

- [1] I. T. Franco, R. M. Figueiredo, "Predictive Maintenance: An Embedded System Approach", *J. control, automation and electrical systems*, 34, 60–72, 2023.
- [2] X. Q. Zhao, S. Guo, Y. Long, G., X. Zhong, "Simultaneous fault detection and control for discrete-time switched systems under relaxed persistent dwell time switching", *Applied Mathematics and Computation*, 412, 26585, 2022.
- [3] X. Liu, Y. Chen, L. Xiong, C. Wang, C. Luo, L. Zhang, K. Wang, "Intelligent fault diagnosis methods toward gas turbine: A review", Withdrawn Article in Press: *Chinese Journal of Aeronautics*, 2023. Doi: 10.1016/j.cja.2023.09.024.
- [4] Y. Yan, L. Wu, X. He, et al, "Adaptive Fault-Tolerant Tracking Control of Uncertain Nonlinear Systems with Event-Triggered Inputs and Full State Constraints", *J. Control, Automation and Electrical Systems*, 33, pp. 1688–1699, 2020.
- [5] K. Telbissi, A. Benzaouia, "Robust Fault Tolerant Control for Uncertain Switched Systems with Time Delay", *J. Control, Automation and Electrical Systems*, 34, pp. 496–506, 2023.
- [6] J. Lan, R. J. Patton, "Robust Integration of Model-Based Fault Estimation and Fault-Tolerant Control", *Advances in Industrial Control*, 2021. Doi: 10.1007/978-3-030-58760-4
- [7] C. Sadhukhan, M. S. Kumar, N. M. Kanti, M. Sharifpur, "Fault diagnosis of a nonlinear hybrid system using adaptive unscented Kalman filter bank", *Engineering with Computers*, 2021. Doi: 10.1007/s00366-020-1235-0
- [8] ص. اکبرپور، م. ج. خسروجرودی "تخمین عیب در محفظه احتراق وکمپرسور توربین های گازی صنعتی به روش چند مدله" نشریه مهندسی شیمی ایران، جلد ۲۳، شماره ۱۳۴ تیر ۱۴۰۲
- [9] M. Soleimani, F. Capman, D. Neagu, "Diagnostics and prognostics for complex systems: A review of methods and challenges", *Quality and Reliability Engineering International*, pp. 1–33, 2021.
- [۱۰] ن. صادق زاده، ب. سلطانی، م. میرزایی، "مشاهدهگرهای متعامل غیرخطی در تشخیص عیبهای حسگری و عملکردی در سیستم ماهواره" مجله مهندسی برق دانشگاه تبریز، جلد ۵۰، شماره ۴، صفحات ۱۷۰۹–۱۷۲۲، ۱۳۹۹
- [۱۱] آ. م. آقازمانی، ج. دلاوری، "کنترل مد لغزشی مرتبه کسری تطبیقی برای ژنراتور مغناطیس دائم سنکرون همراه با رویکرد اغتشاش" مجله مهندسی برق دانشگاه تبریز، جلد ۵۲، شماره ۱، ۱۴۰۱
- [12] S. Venkateswaran, C. Kravaris, "Design of linear unknown input observers for sensor fault estimation in nonlinear systems", *Automatica*, Vol 155, 111152, 2023.
- [13] F. Zhu, Y. Shan, Y. Tang, "Actuator and Sensor Fault Detection and Isolation for Uncertain Switched Nonlinear System Based on Sliding Mode Observers", *J. Control, Automation and Electrical Systems*, 19, 3075–3086, 2021.
- [14] Q. Yang, S. Li, Y. Cao, "Multiple model-based detection and estimation schemes for gas turbine sensor and gas path fault simultaneous diagnosis", *J. Mechanical Science and Technology*, 33 (4): pp. 1959-1972, 2019.
- [15] B. Pourbabaei, N. Meskin, & K. Khorasani, "Robust sensor fault detection and isolation of gas turbine engines subjected to time-varying parameter uncertainties", *Mechanical Systems and Signal Processing*, 76-77, 136–156, 2016.
- [16] J. Y. Keller, M. Darouach, "Fault isolation filter design for linear stochastic systems with unknown inputs". *Proceedings of the 37th IEEE Conference on Decision and Control* (Cat. No.98CH36171), Tampa, FL, USA, vol.1; pp. 598-603, 1998.
- [17] M. Rodrigues, D. Theilliol, M. Adam-Medina, et al, "A fault detection and isolation scheme for industrial systems based on multiple operating models", *J. control engineering practice*, 16; pp. 225–29, 2008.
- [18] R. Makam, K. George, "Convex combination of multiple models for discrete-time adaptive control", *Inter. J. of Systems Science*, 53(4): pp. 743-756, 2022.
- [19] M. Höge, A. Guthke, W. Nowak, "Bayesian Model Weighting: The Many Faces of Model Averaging", *Water*, 12 (2); 309, 2020.
- [20] E. Tavasolipour, J. Poshtan, S. Shamaghdari, "A new approach for robust fault estimation in nonlinear systems with state-coupled disturbances using dissipativity theory", *ISA Transactions*, 114; pp. 31–43, 2021.
- [21] R. Sun, L. Shi, X. Yang, Y. Wang, Q. Zhao, "A coupling diagnosis method of sensors faults in gas turbine control system", *Energy*, 205, 2020.

[22] O. Khustochka, S. Yepifanov, R. Zelenskyi, et al, "Estimation of Performance Parameters of Turbine Engine Components Using Experimental Data in Parametric Uncertainty Conditions", *Aerospace*, 7(1); 6, 2020.

[23] J. Chen, Z. Hu, J. Wang, "Aero-Engine Real-Time Models and Their Applications", *Mathematical Problems in Engineering*, Article ID 9917523, 2021.

[24] A. Nasiri, F. Bayat, S. Mobayen, et al, "Turbines Power Regulation Subject to Actuator Constraints, Disturbances, and Measurement Noises", *IEEE Access*, 9; pp. 40155-40164, 2021.

[25] Q. Yang, Y. Cao, Yet al, "Health Estimation of Gas Turbine: A Symbolic Linearization Model Approach", *ASME Proc. Turbo Expo*, GT2017-64071, 2017.

[26] E. Skeli, D. Weidemann, "Multiple-Model Based Fault-Diagnosis: An Approach to Heterogeneous State Spaces", 23rd International Conference on Methods & Models in Automation & Robotics (MMAR). 2018, Doi:10.1109/mmar.2018.8485836,

[27] H. Yu, Y. Yuecheng, Z. Shiyang, et al, "Comparison of Linear models for gas turbine performance", *Proc IMechE Part G: J. Aerospace Engineering*, 228(8); pp. 1291-1301, 2014.

## Appendix

**Datumn:** Gas turbine's coefficients, linear state space and fault distribution matrices, Transfer filters matrices, and noises in discreet time base at the selected operating points are as:

$J_1=2500 \text{ kg.m}^2$ ,  $j_2=330 \text{ kg.m}^2$ ,  $K=0.98$ ,  $\Gamma=0.25$ ,  $V_1=0.04 \text{ m}^3$ ,  $V_2=0.039 \text{ m}^3$ ,  $V_3=0.023 \text{ m}^3$ ,  $c_{vg}=1.013 \text{ kj/kg}$ ,  $c_{va}=1.042 \text{ kj/kg}$ ,  $c_{pg}=1.75 \text{ kj/kg}$ ,  $H_0=1$ ,  $\eta_{cc}=98 \%$ ,  $\eta_{pr}=80 \%$ ,  $\text{LHV}=50 \text{ Mj/kg}$ ,  $P_5=0.81 \text{ Bar}$ .

$\mathbf{C}_i = \mathbf{I}_6$ ,  $\mathbf{A}_i^{fi} = -10 \text{diag} [1 \ 2 \ 3 \ 4 \ 5 \ 6]$ ,  $\mathbf{B}_i^{fi} = \mathbf{I}_6$ ,  $\mathbf{C}_i^{fi} = \mathbf{I}_6$ ,  $\mathbf{Q}_i = \mathbf{I}_6$ ,  $\mathbf{R}_i = 3 \times \mathbf{I}_6$ ,  $\mathbf{Q}_i' = 0.01 \times \text{diag}[\mathbf{X}_e^i]$ ,  $\mathbf{R}_i' = 0.02 \times \text{diag}[\mathbf{Y}_e^i]$ ,  $\mathbf{O}_2^i = \mathbf{I}_{6 \times 12}$ ,  $\mathbf{O}_2 = \mathbf{I}_{6 \times 12}$

$$\mathbf{A}_1 = \begin{bmatrix} 9998 & 0 & 0 & 1 & -2 & 0 \\ 1 & 9995 & 0 & 3 & 73 & 254 \\ -1 & 0 & 9999 & 0 & 0 & 0 \\ -632 & 0 & 95 & 9058 & -529 & -9 \\ 332 & -7 & 4 & 898 & 9982 & 348 \\ 7 & -384 & -15 & 18 & 382 & 9225 \end{bmatrix} \times 10^{-4}$$

$$\mathbf{A}_2 = \begin{bmatrix} 9998 & 0 & 0 & 01 & -2 & 0 \\ 1 & 9994 & 0 & 4 & 79 & 274 \\ -2 & 0 & 9999 & 0 & 0 & 0 \\ -711 & 0 & 108 & 8950 & -588 & -12 \\ 367 & -9 & 5 & 995 & 9977 & 387 \\ 8 & -423 & -14 & 22 & 421 & 9163 \end{bmatrix} \times 10^{-4}$$

$$\mathbf{A}_3 = \begin{bmatrix} 9997 & 0 & 0 & 1 & -2 & 0 \\ 2 & 9994 & 0 & 4 & 83 & 290 \\ -1 & 0 & 9999 & 0 & 0 & 0 \\ -729 & 0 & 119 & 8936 & -595 & -12 \\ 369 & -9 & 6 & 1005 & 9976 & 393 \\ 8 & -012 & -15 & 21 & 410 & 9249 \end{bmatrix} \times 10^{-4}$$

$$\mathbf{A}_4 = \begin{bmatrix} 9997 & 0 & 0 & 1 & -3 & 0 \\ 2 & 9993 & 0 & 5 & 96 & 338 \\ -1 & 0 & 9999 & 0 & 0 & 0 \\ -705 & 0 & 135 & 8962 & -581 & -12 \\ 362 & -7 & 7 & 983 & 9977 & 384 \\ 8 & -405 & -14 & 20 & 403 & 9334 \end{bmatrix} \times 10^{-4}$$

$$\mathbf{B}_1 = \begin{bmatrix} 0 & -111 & 0 \\ 8 & 6 & 129 \\ 0322 & 3 & 0 \\ 98 & -43 & 76 \\ -3585 & 1809 & -2842 \\ -32 & 32 & 3014 \end{bmatrix} \times 10^{-4}$$

$$\mathbf{B}_2 = \begin{bmatrix} 1 & -123 & 0 \\ 4 & 8 & 141 \\ 341 & 2 & 0 \\ 122 & -56 & 95 \\ -3999 & 2108 & -3163 \\ 44 & 43 & 3314 \end{bmatrix} \times 10^{-4}$$

$$\mathbf{B}_3 = \begin{bmatrix} 1 & -147 & 0 \\ 2 & 8 & 145 \\ 270 & 2 & 0 \\ 124 & -56 & 98 \\ -4040 & 2038 & -3197 \\ -42 & 42 & 3224 \end{bmatrix} \times 10^{-4}$$

$$\mathbf{B}_4 = \begin{bmatrix} 1 & -158 & 0 \\ 1 & 9 & 165 \\ 269 & 2 & 0 \\ 119 & -53 & 93 \\ -3944 & 1990 & -3124 \\ -41 & 41 & 3172 \end{bmatrix} \times 10^{-4}$$

$$\mathbf{E}_1 = \begin{bmatrix} 8 & -129 & 2 \\ 9 & 0 & 5 \\ -98 & 0 & 94 \\ 75726 & 0.0004 & 45785 \\ 3627 & -2 & 1295 \\ 84 & 0 & 29 \\ 11 & -160 & 3 \\ 13 & 0 & 8 \end{bmatrix} \times 10^{-4}$$

$$\mathbf{E}_2 = \begin{bmatrix} -140 & 0 & 135 \\ 92983 & 6 & 61218 \\ 4979 & -3 & 3278 \\ 72 & 0 & 47 \end{bmatrix} \times 10^{-4}$$

$$\mathbf{E}_3 = \begin{bmatrix} 13 & -170 & 4 \\ 14 & 0 & 11 \\ -131 & 0 & 126 \\ 99384 & 6 & 72154 \\ 5378 & -3 & 3904 \\ 76 & 0 & 55 \end{bmatrix} \times 10^{-4}$$

$$\mathbf{E}_4 = \begin{bmatrix} 015 & -0182 & 05 \\ 19 & 0 & 013 \\ -140 & 0 & 134 \\ 113561 & 7 & 76965 \\ 5998 & -3 & 4065 \\ 83 & 0 & 56 \end{bmatrix} \times 10^{-4}$$

$$\mathbf{F}_1^T = [5228 \ 0 \ 1 \ 382 \ 0 \ 0] \times 10^{-4}$$

$$\mathbf{F}_2^T = [18529 \ 0 \ 1 \ 418 \ 0 \ 0] \times 10^{-4}$$

$$\mathbf{F}_3^T = [36794 \ 0 \ 1 \ 442 \ 0 \ 0] \times 10^{-4}$$

$$\mathbf{F}_4^T = [29780 \ 0 \ 1 \ 518 \ 0 \ 0] \times 10^{-4}$$